

Complex 2D Matrix Model and Geometrical Map on Complex- N_c Plane

Kanabu Nawa^{1,*}, Sho Ozaki^{1,2}, Hideko Nagahiro^{3,4}, Daisuke Jido^{5,6}, and Atsushi Hosaka⁴

¹*Quantum Hadron Physics Laboratory, RIKEN Nishina Center, Saitama 351-0198, Japan*

²*Institute of Physics and Applied Physics, Yonsei University, Seoul 120-749, Korea*

³*Department of Physics, Nara Women's University, Nara 630-8506, Japan*

⁴*Research Center for Nuclear Physics (RCNP), Osaka University, Osaka 567-0047, Japan*

⁵*Yukawa Institute for Theoretical Physics, Kyoto University, Kyoto 606-8502, Japan*

⁶*J-PARC Branch, KEK Theory Center, Institute of Particle and Nuclear Studies, Ibaraki 319-1106, Japan*

**E-mail: knawa@riken.jp*

.....
 We study the parameter dependence of the internal structure of resonance states by formulating Complex two-dimensional (2D) Matrix Model, where the two dimensions represent two-levels of resonances. We calculate a critical value of the parameter at which “nature transition” with character exchange occurs between two resonance states, from the viewpoint of geometry on complex-parameter space. Such critical value is useful to know the internal structure of resonance states with variation of the parameter in the system. We apply the model to analyze the internal structure of hadrons with variation of the color number N_c from ∞ to a realistic value 3. By regarding $1/N_c$ as the variable parameter in our model, we calculate a critical color number of nature transition between hadronic states in terms of quark-antiquark pair and mesonic molecule as exotics from the geometry on complex- N_c plane. For the large- N_c effective theory, we employ the chiral Lagrangian induced by holographic QCD with D4/D8/ $\overline{D8}$ multi-D brane system in the type IIA superstring theory.

Subject Index D32

1. Introduction

How do characters of states change with variation of a parameter which specifies the property of the system or of the environment where the system is placed? This is a general issue discussed in various phenomena of physics; deformed nuclei depending on the deformation parameter of nuclear mean-field potential [1], electronic wave function configurations of diatomic molecules depending on the internuclear distance [2], and conversion of solar neutrinos depending on the distance from the center of the sun [3]. In quantum mechanics, one starts with a Hermite model Hamiltonian $\hat{H}(\lambda)$ with a real parameter λ . Here one can assume that the eigenstates ϕ_i ($i = 1, 2, \dots$) of $\hat{H}(\lambda)$ at $\lambda = 0$ can be an appropriate basis with clear characters to classify the properties of the eigenstates $\psi_i(\lambda)$ ($i = 1, 2, \dots$) for finite λ . Now, if the energy expectation values $\varepsilon_i(\lambda) \equiv \langle \phi_i | \hat{H}(\lambda) | \phi_i \rangle$ ($i = 1, 2, \dots$) cross with each other at a certain value $\lambda = \lambda_t \in \mathbf{R}$, the energy eigenvalues $E_i(\lambda)$ of $\psi_i(\lambda)$ with finite mixing have level repulsion, i.e., anticrossing at λ_t (see Fig. 1(a)) due to the Neumann-Wigner non-crossing rule [4]. At this point, the overlap between $\psi_i(\lambda)$ and ϕ_i is exceeded by

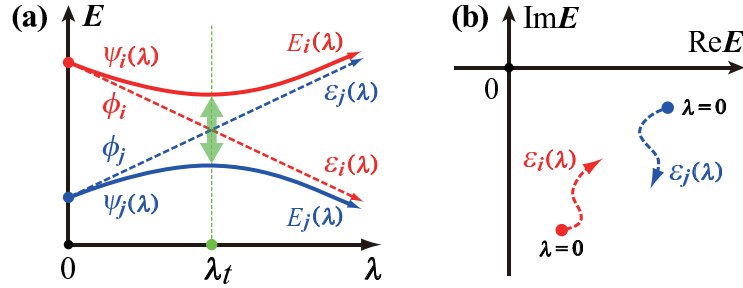


Fig. 1 (Color) (a) Anticrossing between i th and j th eigenstates of Hermite Hamiltonian $\hat{H}(\lambda)$ with variation of $\lambda \in \mathbf{R}$. Indices of lines are explained in the text. i th and j th eigenstates exchange their characters at anticrossing point $\lambda = \lambda_t$ as the nature transition. (b) $\varepsilon_i(\lambda)$ and $\varepsilon_j(\lambda)$ of non-Hermite Hamiltonian $\hat{H}(\lambda)$ with variation of $\lambda \in \mathbf{R}$ on complex energy plane. $\varepsilon_i(\lambda)$ and $\varepsilon_j(\lambda)$ generally have no degeneracy at certain value of $\lambda \in \mathbf{R}$ except for accidental case.

that between $\psi_i(\lambda)$ and ϕ_j ($i \neq j$) as $|\langle \phi_i | \psi_i \rangle|^2 \leq |\langle \phi_j | \psi_i \rangle|^2$. Therefore, due to orthogonality, $\psi_i(\lambda)$ and $\psi_j(\lambda)$ exchange their characters in terms of the appropriate basis ϕ_i and ϕ_j at the anticrossing point $\lambda = \lambda_t$, which we call “nature transition” in this paper. In fact, the critical value λ_t is very useful to know the internal structure of the quantum states with variation of certain parameter λ .

In this paper, we consider the quantum systems with dissipation into decay channels outside of the model space. Such systems are often called *open quantum systems* with resonance states, which are effectively described by a non-Hermite model Hamiltonian $\hat{H}(\lambda)$ with complex energy eigenvalues [5]. The real and imaginary parts of the eigenvalues correspond to the mass and decay width of the resonance states, respectively. It can be shown in the Feshbach reduction formalism that the Hamiltonian with a reduced model space becomes non-Hermitian [6–8]. In such open quantum systems, $\varepsilon_i(\lambda)$ of ϕ_i can move on the complex energy plane (see Fig. 1(b)) without having degeneracy at a certain value of λ except for an accidental case [9]. Therefore, a simple criterion should be newly found to judge the existence of the nature transition between the resonances, and its critical value λ_t can be used to know the internal structure of the resonance states depending on the parameter. In this paper, we construct Complex two-dimensional (2D) Matrix Model to discuss the nature transition between two resonance states. (Two dimensions represent two levels of resonances.) This 2D model will give an elementary understanding for higher dimensional problems because the latter can often be reduced locally to the 2D problems. We show that, by extending λ to a *complex variable*, the geometry on the complex- λ plane gives a criterion of the nature transition within the real parameter subspace $\lambda \in \mathbf{R}$.

After establishing the general framework, we apply it to the hadron physics with strong interaction, which is governed by *quantum chromodynamics* (QCD) as the $SU(N_c)$ gauge theory with color number $N_c = 3$ [10]. By extending N_c to an arbitrary number, $1/N_c$ -expansion provides a systematic perturbative treatment. The leading order of “large- N_c QCD” reproduces lots of QCD phenomenologies [11, 12]. In fact, in large- N_c QCD, the internal structure of mesons becomes clear: mesons as quark-antiquark ($q\bar{q}$) pairs appear with masses of $O(N_c^0)$ and zero widths, while “mesonic molecules” can also appear as resonances with masses and

widths increasing along with N_c because the meson-meson interactions are suppressed with $O(1/N_c)$ [13]. From such considerations in large- N_c , one often expects that exotics can also be suppressed in the real world [12]. However the internal structures of hadrons can be easily changed due to the development of hadron dynamics scaled by $1/N_c$. Here, a basic but essential question arises: *what is the internal structure of hadrons with continuous variation of N_c from ∞ to 3?* To find a typical feature for such N_c -dependence of the internal structure of hadrons, we adopt the Complex 2D Matrix Model. By regarding $q\bar{q}$ and mesonic molecule states in large- N_c as the appropriate basis ϕ_i ($i = 1, 2$) with clear characters, and by identifying $1/N_c$ to λ in the Complex 2D Matrix Model, we will calculate a critical color number of nature transitions in terms of appropriate basis from the geometry on the complex- N_c plane. As an example, we investigate the internal structure of $a_1(1260)$ meson with admixed nature of $q\bar{q}$ and $\pi\rho$ -molecule components. For the large- N_c effective theory, we employ the chiral Lagrangian induced by holographic QCD with D4/D8/ $\overline{D8}$ multi-D brane system in the type IIA superstring theory [14, 15].

In Sec. 2, we formulate Complex 2D Matrix Model. In Sec. 3, we discuss the application of the model to N_c -dependence of internal structure of hadrons. Sec. 4 is devoted to summary and outlook. In Appendix A, we calculate the attaching number N_{at} which characterizes the geometry near the origin on the complex-parameter space. In Appendix B, we show a simple prescription of writing geometrical maps for arbitrary matrix elements of the model.

2. Complex 2D Matrix Model

First we formulate Complex 2D Matrix Model to treat a two-level problem in a quantum system with resonances. We describe resonance states by using the bi-orthogonal representation as $|\phi_i\rangle$ ($i = 1, 2$): its bra-state is defined by the complex conjugate of the Dirac bra-state ($\langle\phi_i| \equiv \langle\phi_i^*$), which was firstly introduced for the unstable nuclei in nuclear physics [16–18]. Only by taking such bi-orthogonal representation, resonance states with different eigenvalues become orthogonal to each other as $(\phi_i|\phi_j) = \delta_{ij}$, which is needed to employ the matrix representation of operators in such basis. As anticipated, we assume that $|\phi_i\rangle$, the eigenstates of $\hat{H}(\lambda)$ at $\lambda = 0$, are the appropriate basis with clear characters and are useful to classify the quantum states. Hence we consider the Hamilton matrix $H(\lambda) \equiv [(\phi_i|\hat{H}(\lambda)|\phi_j)]$ in this basis:

$$H(\lambda) = \begin{pmatrix} \varepsilon_1(\lambda) & V_{12}(\lambda) \\ V_{21}(\lambda) & \varepsilon_2(\lambda) \end{pmatrix}, \quad (1)$$

where $\varepsilon_i(\in \mathbf{C})$ is the energy of $|\phi_i\rangle$ and $V_{ij}(\in \mathbf{C})$ are the interaction satisfying $V_{ij}(0) = 0$. $\lambda(\in \mathbf{R})$ is a parameter, controlling the development of the two eigenstates $|\psi_i(\lambda)\rangle$ which can be obtained in terms of the basis $|\phi_i\rangle$ as

$$|\psi_i(\lambda)\rangle \equiv C_{i1}(\lambda)|\phi_1\rangle + C_{i2}(\lambda)|\phi_2\rangle. \quad (i = 1, 2) \quad (2)$$

The coefficients $C_{ij}(\lambda)$ carry the information for the internal structure of the eigenstates $|\psi_i(\lambda)\rangle$ in terms of $|\phi_i\rangle$. There is a subtlety for the interpretation of component weights from $C_{ij}(\lambda)$, since the norms $(\psi_i|\psi_i) = C_{i1}^2 + C_{i2}^2$ can be complex numbers due to the bi-orthogonality. Several attempts have been made to interpret such complex probability of resonances (for example, see Ref. [19]), while a consensus has not been achieved yet. Recently Ref. [20] has considered a probabilistic interpretation of resonance states by taking the

integral of the modulus square of resonance wave function over a limited spatial domain expanding with the speed of leaking particles. Normalization of the resonance wave function over such domain makes the modulus square finite and could be suitable for the probabilistic interpretation. However, as for the expansion coefficients in Eq. (2), their probabilistic interpretation still remains unsolved. In this work we simply presume the module, $|C_{ij}(\lambda)|^2$, to be interpreted as the component weights, as it is suitable for narrow resonances. At $\lambda = 0$, $|\psi_i(\lambda)$ coincides with $|\phi_i)$ due to $V_{ij}(0) = 0$, so that $C_{ij}(0) = 0$ for $i \neq j$.

Now, if $\hat{H}(\lambda)$ is Hermite with real eigenvalues, the level crossing of $|\phi_i)$ is known to give the level anticrossing of $|\psi_i(\lambda)$ as shown in Fig. 1(a) [4]. At this anticrossing point $\lambda = \lambda_t$, $|\psi_i(\lambda)$ exchange their characters as “nature transition” with the transition condition $|C_{i1}(\lambda_t)|^2 = |C_{i2}(\lambda_t)|^2$, where the two basis components $|\phi_1)$ and $|\phi_2)$ are equally mixed as a character exchanging point. In this paper, we newly consider the case that $\hat{H}(\lambda)$ is non-Hermite with complex eigenvalues for resonance states. As we will show below, $|C_{i1}|^2 = |C_{i2}|^2$ can be satisfied *at least* by the energy coincidence $E_1 = E_2$, which can be realized if one extends λ to a *complex variable* [21]. Therefore, to get a geometrical insight for the existence of nature transition, here we introduce the *complex- λ plane*.

By solving the Schrödinger equation: $\hat{H}|\psi\rangle = E|\psi\rangle$, we find the two eigenvalues $E_i(\lambda)$ ($i = 1, 2$) as

$$E_i(\lambda) = \{\varepsilon_1(\lambda) + \varepsilon_2(\lambda)\}/2 \pm F(\lambda), \quad (3)$$

$$F(\lambda) \equiv \sqrt{A(\lambda)^2 + \bar{V}(\lambda)^2}, \quad (4)$$

$$A(\lambda) \equiv \{\varepsilon_1(\lambda) - \varepsilon_2(\lambda)\}/2, \quad (5)$$

$$\bar{V}(\lambda)^2 \equiv V_{12}(\lambda)V_{21}(\lambda), \quad (6)$$

and the coefficient ratios $R_i(\lambda)$ of the eigenstates $|\psi_i(\lambda)$ ($i = 1, 2$) in Eq. (2) as

$$R_i(\lambda) \equiv \frac{C_{i2}(\lambda)}{C_{i1}(\lambda)} = -\frac{1}{V_{12}(\lambda)}\{A(\lambda) \mp F(\lambda)\}. \quad (7)$$

The upper (lower) sign in Eqs. (3) and (7) corresponds to $i = 1$ ($i = 2$). The ratios (7) are sufficient to discuss the nature transition between two levels as below. Now we consider the transition condition $|C_{i1}(\lambda)|^2 = |C_{i2}(\lambda)|^2$ on the complex- λ plane. Due to the bi-orthogonality $(\psi_1|\psi_2) = 0$, i.e., $R_1R_2 = -1$, the transition condition can be written only by the ratios (7) as $|R_1(\lambda)| = |R_2(\lambda)|$, which is equivalent from Eq. (7) to

$$\text{Re}[A(\lambda)^*F(\lambda)] = 0. \quad (8)$$

Due to the square root in (4), Eq. (8) becomes equivalent to the two conditions:

$$\text{Re}[A(\lambda)^*\bar{V}(\lambda)] = 0, \quad (9)$$

$$|A(\lambda)|^4 - \{\text{Im}[A(\lambda)^*\bar{V}(\lambda)]\}^2 \leq 0. \quad (10)$$

From Eq. (9), $|\text{Im}[A(\lambda)^*\bar{V}(\lambda)]| = |A(\lambda)||\bar{V}(\lambda)|$, so that the condition (10) becomes

$$|A(\lambda)|^2 \leq |\bar{V}(\lambda)|^2, \quad (11)$$

which has been divided by $|A(\lambda)|^2$ since λ 's for $A(\lambda) = 0$ trivially satisfy the conditions (9) and (11). Now the “transition line” is defined as the region satisfying $|C_{i1}(\lambda)|^2 = |C_{i2}(\lambda)|^2$, i.e., both conditions (9) and (11) on the complex- λ plane. Therefore, the line (9), named

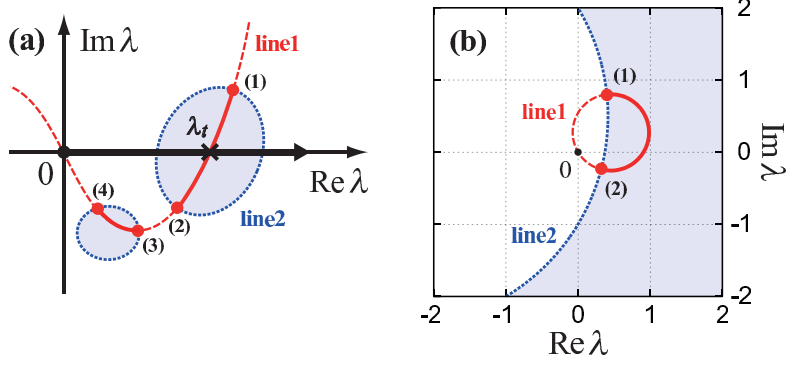


Fig. 2 (Color) (a) Schematic figure of geometrical map with transition lines and exceptional points on complex λ plane. Line 1 and shaded area with boundary of line 2 correspond to the conditions (9) and (11), respectively. Points (n) denote the exceptional points $\lambda_{\text{EX}}^{(n)}$. Transition lines are shown by the solid curves, which satisfy both (9) and (11). (b) Linear- λ model with $\varepsilon_1^{(0)} = 1000 - 200i$, $\varepsilon_2^{(0)} = 1200$, $v_{11} = 100 + 100i$, $v_{22} = -100 - 200i$, $v_{12} = v_{21} = 200 + 50i$ in MeV unit as test values.

“line 1”, can be the candidate of the transition line, and the region (11) with the boundary $|A(\lambda)|^2 = |\overline{V}(\lambda)|^2$, named “line 2”, selects the proper part for the transition line. The region (11) always excludes the origin $\lambda = 0$ for the case $\varepsilon_1(0) \neq \varepsilon_2(0)$, because $|A(0)| > 0$ and $|\overline{V}(0)| = 0$. Then, if the transition line crosses the real- λ axis, the nature transition occurs at the crossing point $\lambda = \lambda_t \in \mathbf{R}$ (see schematic Fig. 2(a)).

Now, from (9) and (11), the crossing points $\lambda = \lambda_{\text{EX}}^{(n)} \in \mathbf{C}$ ($n = 1, 2, \dots$) of line 1 and line 2 satisfy the condition $A(\lambda) * F(\lambda) = 0$ for $\forall A(\lambda) \neq 0$, which is equivalent to

$$F(\lambda)^2 = A(\lambda)^2 + \overline{V}(\lambda)^2 = 0. \quad (12)$$

Therefore, at $\lambda = \lambda_{\text{EX}}^{(n)}$, the mass difference in Eq. (3) becomes zero and two eigenvalues coincide as $E_1(\lambda) = E_2(\lambda)$. $\lambda_{\text{EX}}^{(n)}$ are called the “exceptional points” on the complex- λ plane [21]. In fact, the importance of the exceptional points has been intensively studied both theoretically [22] and experimentally [23] in the area of quantum chaos, where the dense exceptional points on the complex- λ plane correspond to the development of quantum chaos in the energy-level statistics [22]. Now, in this paper, we can show that line 1 and line 2 cross each other at all exceptional points, so that these points can always be the *end points* of the transition lines. Therefore, the location of the exceptional points is very important to geometrically judge the existence of $\lambda_t \in \mathbf{R}$.

One simple example is the “linear- λ model” with Hamilton matrix:

$$H(\lambda) = \begin{pmatrix} \varepsilon_1^{(0)} & 0 \\ 0 & \varepsilon_2^{(0)} \end{pmatrix} + \begin{pmatrix} \lambda v_{11} & \lambda v_{12} \\ \lambda v_{21} & \lambda v_{22} \end{pmatrix}, \quad (13)$$

where $\varepsilon_i^{(0)}$ and v_{ij} ($i, j = 1, 2$) are λ -independent quantities. Two exceptional points and one transition line appear (see Fig. 2(b)), which are simply checked from the power counting about λ in (12). In this model, Eq. (9) can be equally written with $\Delta\varepsilon \equiv \varepsilon_1^{(0)} - \varepsilon_2^{(0)}$, $\Delta v \equiv v_{11} - v_{22}$,

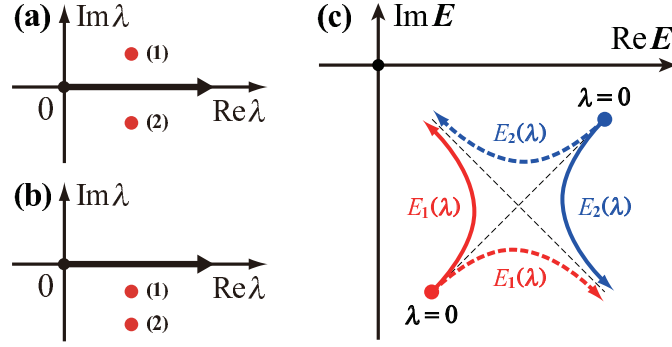


Fig. 3 (Color) Two exceptional points on complex- λ plane; (a) two locate on the opposite side striding over the real- λ axis, and (b) two locate without striding it. Bold arrow implies the variation of λ within real parameter subspace. (c) Eigenvalue behaviors on the complex energy plane with level anticrossing/width crossing shown by the solid lines and level crossing/width anticrossing shown by the dashed lines.

and $\bar{v}^2 \equiv v_{12}v_{21}$ as

$$|\lambda - \bar{\lambda}| = |\bar{\lambda}|, \quad (\bar{\lambda} \equiv -(\Delta\varepsilon)\bar{v}^*\{2\text{Re}[(\Delta v)\bar{v}^*]\}^{-1}) \quad (14)$$

so that line 1 is a circle crossing at $\lambda = 0$, $\lambda_{\text{EX}}^{(1)}$ and $\lambda_{\text{EX}}^{(2)}$, and the transition line has an arc shape. Ref. [22] shows that, in the linear- λ model, the eigenvalue behaviors for $\lambda \in \mathbf{R}$ depend on the location of the two exceptional points; if the two locate on the opposite sides striding over the real- λ axis (see in Fig. 3(a)), level anticrossing/width crossing occurs, while, if not (see Fig. 3(b)), level crossing/width anticrossing occurs as in Fig. 3(c). Therefore, by comparing Fig. 2(b) and Fig. 3, we can newly suggest that the nature transition occurs only in the level anticrossing/width crossing case. In this way, as for the linear- λ model with two exceptional points, we can relate the behaviors of poles on the complex-energy plane and their internal structures through the geometry on the complex- λ plane. The linear- λ model also suggests that, if $v_{11} = v_{22} = 0$, the radius of the circle of line 1 in Eq. (14) diverges: $|\bar{\lambda}| \rightarrow \infty$, so that there is no nature transition for finite λ . There only occurs the mixing of the basis components up to 50% at most. Therefore the λ -dependence in the diagonal components of the matrix form (1) is needed to have the nature transition between resonance states.

We can show more general cases of the geometrical map as the “ PQR model” by using the following matrix:

$$H(\lambda)_{PQR} = \begin{pmatrix} \varepsilon_1^{(0)} & 0 \\ 0 & \varepsilon_2^{(0)} \end{pmatrix} + \begin{pmatrix} \lambda^P v_{11} & \lambda^R v_{12} \\ \lambda^R v_{21} & \lambda^Q v_{22} \end{pmatrix}, \quad (15)$$

where P, Q and R are the powers of λ in the matrix elements. As examples, geometrical maps of H_{221}, H_{233} and H_{151} with $\varepsilon_i^{(0)}$ and v_{ij} fixed are presented in Fig. 4. By changing the values of P, Q and R , various types of geometry can be observed on the complex- λ plane. Fig. 4 and Fig. 2(b) classified as H_{111} also show that the geometry around $\lambda = 1$ is rather independent of the values of P, Q and R with the same values of $\varepsilon_i^{(0)}$ and v_{ij} . On the other hand, H_{001} effectively corresponds to the linear- λ model with $v_{11} = v_{22} = 0$, so that there is no nature transition for finite λ as discussed below Eq. (14). (If $\varepsilon_i^{(0)}$ and v_{ij} ($i, j = 1, 2$) are specially chosen for line 1 to exactly cross the point $\lambda = 1$, H_{001} still corresponds to the

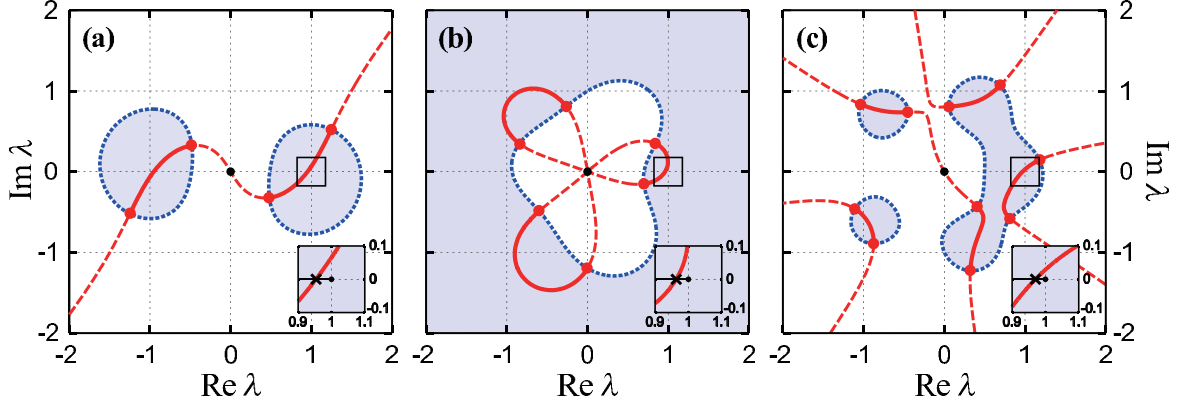


Fig. 4 (Color) Geometrical maps of (a) H_{221} , (b) H_{233} and (c) H_{151} with $\varepsilon_1^{(0)} = 1000 - 200i$, $\varepsilon_2^{(0)} = 1200$, $v_{11} = 100 + 100i$, $v_{22} = -100 - 200i$, $v_{12} = v_{21} = 200 + 50i$ in MeV unit as test values. Notations for line 1, line 2, exceptional points and transition lines are same as those in Fig. 2(a). Blank squares show the area around $\lambda = 1$.

linear- λ model with $v_{11} = v_{22} = 0$ where line 1 as a circle of infinite radius coincides with the real- λ axis itself.) These features can be roughly understood as follows; First, let us consider a situation that line 1 of Eq. (9) appears near $\lambda = 1$, i.e., Eq. (9) is satisfied at $\lambda = 1 + \xi$ ($\exists \xi \in \mathbf{C}, |\xi| \ll 1$) as

$$\text{Re} \left[\left\{ \Delta\varepsilon + (1 + \xi)^P v_{11} - (1 + \xi)^Q v_{22} \right\}^* (1 + \xi)^{R\bar{v}} \right] = 0, \quad (16)$$

with $\Delta\varepsilon \equiv \varepsilon_1^{(0)} - \varepsilon_2^{(0)}$ and $\bar{v}^2 \equiv v_{12}v_{21}$. LHS of Eq. (16) can be expanded up to $O(\xi^1)$ as

$$\text{Re} [(\Delta\varepsilon + \Delta v)^* \bar{v}] + \text{Re} [\xi^* v_{11}^* \bar{v}] P - \text{Re} [\xi^* v_{22}^* \bar{v}] Q + \text{Re} [(\Delta\varepsilon + \Delta v)^* \xi \bar{v}] R = 0, \quad (17)$$

with $\Delta v = v_{11} - v_{22}$. Eq. (17) implies that, with increase of $|P|$, $|Q|$ and $|R|$, $|\xi|$ tends to decrease to maintain Eq. (17). That is, a part of line 1 approaches asymptotically to $\lambda = 1$ as its “fixed point”. Actually, $|P|$, $|Q|$ and $|R|$ determine, via Eq. (17), the order of $|\xi|$. Furthermore, line 1 always crosses the point $\lambda = 0$ for $R > 0$ (see Appendix A), so that $|\xi|$ should be *at least* $O(1)$ or *less* for any powers with $R > 0$. Therefore, $|P|$, $|Q|$ and $|R|$ which are *sufficiently larger than unity* tend to develop a power-independent geometry of line 1 in the vicinity of $\lambda = 1$ in comparison to a length scale $O(1)$ on the complex- λ plane.

So far, we have formulated the model described by the Hamiltonian (1) with arbitrary complex functions: $\varepsilon_i(\lambda)$ and $V_{ij}(\lambda)$, and studied two-level problems on the complex-energy plane. We have shown that the geometrical map on the complex- λ plane provides the geometrical insight for the existence of nature transition within the real parameter subspace $\lambda \in \mathbf{R}$. For convenience, we supply in Appendix B a prescription of writing geometrical maps for arbitrary $\varepsilon_i(\lambda)$ and $V_{ij}(\lambda)$, instead of numerically solving the high-powered algebraic equations (9) and (11).

3. Application to N_c -dependence of internal structure of hadrons

Let us now utilize the Complex 2D Matrix Model to find the typical N_c -dependence of the internal structure of hadrons. As a demonstration, we consider the $a_1(1260)$ meson which has admixed nature of $q\bar{q}$ and $\pi\rho$ -molecule components. First, we prepare the appropriate

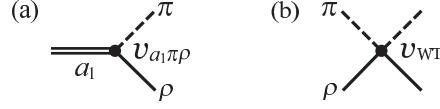


Fig. 5 Interactions between π , ρ and a_1 mesons; (a) three-point interaction and (b) Weinberg-Tomozawa interaction.

basis for the $q\bar{q}$ and the $\pi\rho$ -molecule states in large- N_c . For the large- N_c effective theory, we make use of the chiral Lagrangian induced by holographic QCD with D4/D8/ $\overline{\text{D8}}$ multi-D brane system in the type IIA superstring theory [14, 15]. Due to the large- N_c condition of the duality with “classical” supergravity, the a_1 meson appearing as a gauge field in holographic QCD should correspond to the $q\bar{q}$ state. On the other hand, the holographic action also induces the energy-dependent π - ρ interaction as the Weinberg-Tomozawa (WT) interaction of order $O(1/N_c)$. Due to its attractive interaction, the non-perturbative π - ρ dynamics gives a resonance pole as the “ $\pi\rho$ -molecule state”. The a_1 meson as the $\pi\rho$ -molecule is also studied in the chiral unitary model [24, 25]. Thus, by preparing the $q\bar{q}$ and $\pi\rho$ -molecule states as the appropriate basis ϕ_i ($i = 1, 2$) and identifying $1/N_c$ to λ in the Complex 2D Matrix Model, we will calculate the critical color number of the nature transition from the geometry on the complex- N_c plane.

Here we investigate the scattering equation for the π - ρ propagator in the $J^P = 1^+$ channel. By reducing the relativistic eigenvalue equation to the Schrödinger equation of the model (1) with a non-relativistic approximation as discussed below, we will derive the geometrical map on the complex- N_c plane for the a_1 meson. From the Lagrangian in holographic QCD [14, 15], we obtain the three-point interaction $v_{a_1\pi\rho}$ and the WT interaction v_{WT} in Fig. 5 after proper s -wave projection [26] in the form,

$$v_{a_1\pi\rho} = \frac{2\sqrt{2}}{f_\pi} g_{a_1\pi\rho} (s - m_\rho^2), \quad (18)$$

$$v_{\text{WT}} = -\frac{1}{4f_\pi^2} \{3s - 2(m_\rho^2 + m_\pi^2) - (m_\rho^2 - m_\pi^2)^2 \frac{1}{s}\}. \quad (19)$$

By taking the two experimental inputs, e.g., $f_\pi = 92.4\text{MeV}$ and $m_\rho = 776\text{MeV}$, all the masses and coupling constants of hadrons can be uniquely determined in the holographic approach as $m_{a_1} = 1189\text{MeV}$ and $g_{a_1\pi\rho} = 0.26$ [14]. (In the D4/D8/ $\overline{\text{D8}}$ model, pion is massless, whereas we use an isospin-averaged mass value: $m_\pi = 138\text{MeV}$.)

Now we introduce a two-dimensional G-function with $\pi\rho$ and $q\bar{q}$ channels, having $J^P = 1^+$ as the a_1 meson:

$$G^{-1} = G_0^{-1} - V \quad (20)$$

$$= \begin{pmatrix} G_{\pi\rho} & 0 \\ 0 & G_{a_1} \end{pmatrix}^{-1} - \begin{pmatrix} v_{\text{WT}} & v_{a_1\pi\rho} \\ v_{a_1\pi\rho} & 0 \end{pmatrix}, \quad (21)$$

where $G_{a_1} \equiv (s - m_{a_1}^2)^{-1}$ is a propagator for the $q\bar{q}$ state as the a_1 meson and $G_{\pi\rho}$ is $\pi\rho$ loop function [24] as

$$G_{\pi\rho} \equiv i \int \frac{d^4q}{(2\pi)^4} \frac{1}{(P-q)^2 - m_\pi^2 + i\epsilon} \frac{1}{q^2 - m_\rho^2 + i\epsilon}, \quad (22)$$

with P a total incident momentum as $P^2 = s$. We use a dimensional regularization with the natural condition [27] to avoid the effect of CDD pole in Eq. (22). In fact, the loop integral of Eq. (22) appears in the scattering equation of the T-matrix with the separable approximation for the interactions [24]. Then one can sum up the diagonal component of the potential in Eq. (21) as

$$G^{-1} = \begin{pmatrix} G_{\text{WT}} & 0 \\ 0 & G_{a_1} \end{pmatrix}^{-1} - \begin{pmatrix} 0 & v_{a_1\pi\rho} \\ v_{a_1\pi\rho} & 0 \end{pmatrix}, \quad (23)$$

with $G_{\text{WT}}^{-1} \equiv G_{\pi\rho}^{-1} - v_{\text{WT}}$. We numerically find that G_{WT} has single resonance pole above the $\pi\rho$ threshold as

$$G_{\text{WT}} = \frac{G_{\pi\rho}}{1 - v_{\text{WT}}G_{\pi\rho}} \equiv \frac{Z(s)}{s - s_p}. \quad (24)$$

This pole appears due to non-perturbative dynamics between π and ρ through the 4-point coupling v_{WT} , so that we interpret $(s - s_p)^{-1}$ in Eq. (24) as the propagator of “ $\pi\rho$ -molecule state” with a wave function renormalization factor $Z(s)$. To renormalize (24), $Z(s)$ can be attached to the interaction sector by $\bar{G}^{-1} \equiv \text{diag}(\sqrt{Z}, 1)G^{-1}\text{diag}(\sqrt{Z}, 1)$ as

$$\bar{G}^{-1} = \begin{pmatrix} s - s_p & 0 \\ 0 & s - m_{a_1}^2 \end{pmatrix} - \begin{pmatrix} 0 & \sqrt{Z}v_{a_1\pi\rho} \\ \sqrt{Z}v_{a_1\pi\rho} & 0 \end{pmatrix}, \quad (25)$$

where the first term is the inverse of the “free” propagator for the $\pi\rho$ -molecule state and the $q\bar{q}$ state as the a_1 meson. Now, by solving the relativistic eigenvalue equation for \bar{G} as

$$\det \bar{G}^{-1} = 0, \quad (26)$$

we have arrived at two-level model for the a_1 meson with the $\pi\rho$ -molecule and the $q\bar{q}$ components having proper mixing.

Now, to get the geometrical map on the complex- N_c plane for the a_1 meson, we reduce Eq. (26) to the Schrödinger equation for Eq. (1), with a non-relativistic approximation. We approximate the molecule propagator and the renormalization factor in Eq. (24) as $(s - s_p)^{-1} \simeq \{2\sqrt{s_p}(E - \sqrt{s_p})\}^{-1}$ and $\sqrt{Z} \simeq 84 - 21i$ estimated at $\sqrt{s} = \sqrt{s_p} \simeq 1012 - 221i$ in MeV unit. We also approximate the $q\bar{q}$ propagator and the coupling constant as $(s - m_{a_1}^2)^{-1} \simeq \{2m_{a_1}(E - m_{a_1})\}^{-1}$ and $v_{a_1\pi\rho} \simeq -6493$ at $\sqrt{s} = m_{a_1} = 1189$ in MeV unit. Such energy fixing has been traditionally employed in nuclear-physics shell-model study, where the absorptive effects into decay channels outside of the model space are represented by the non-Hermite matrix elements [18]. Then, Eq. (26) can be written as

$$(E - \sqrt{s_p})(E - m_{a_1}) - \frac{1}{(2\tilde{m})^2}(\sqrt{Z}v_{a_1\pi\rho})^2 = 0, \quad (27)$$

with $\tilde{m} \equiv \sqrt{\sqrt{s_p}m_{a_1}}$. From the Schrödinger equation (27), we can construct the two dimensional Hamilton matrix as

$$H = \begin{pmatrix} \sqrt{s_p} & \frac{1}{2\tilde{m}}\sqrt{Z}v_{a_1\pi\rho} \\ \frac{1}{2\tilde{m}}\sqrt{Z}v_{a_1\pi\rho} & m_{a_1} \end{pmatrix}. \quad (28)$$

Now we evaluate N_c -counting for the matrix elements in Eq. (28). According to large- N_c QCD [11, 12], m_{a_1} , $v_{a_1\pi\rho}$ and $G_{\pi\rho}$ [28] have N_c -dependence as

$$m_{a_1} \sim O(N_c^0), \quad v_{a_1\pi\rho} \sim O(1/\sqrt{N_c}), \quad G_{\pi\rho} \sim O(N_c^0). \quad (29)$$

For energy region far from the threshold; $s \gg (m_\rho + m_\pi)^2$, the Weinberg-Tomozawa interaction (19) can be simplified as $v_{\text{WT}} \sim s \times O(1/N_c)$ as the mesonic four-point interaction [11, 12]. Therefore, Eq. (24) can be rewritten as

$$G_{\text{WT}} \sim \frac{G_{\pi\rho}}{1 - \{s \times O(1/N_c)\}G_{\pi\rho}} \sim \frac{O(N_c)}{s - O(N_c)/G_{\pi\rho}}. \quad (30)$$

By comparing Eqs.(24) and (30), we can also estimate the N_c dependence of $\sqrt{s_p}$ and \sqrt{Z} as

$$\sqrt{s_p} \sim O(\sqrt{N_c}), \quad \sqrt{Z} \sim O(\sqrt{N_c}), \quad (31)$$

where energy dependence of the loop function $G_{\pi\rho}$ is approximately ignored. Such increasing behavior of $\sqrt{s_p}$ with N_c as in Eq. (31) can also be observed in the second reference of [13]. By using Eq. (31), we can also estimate the N_c -dependence of energy scale \tilde{m} introduced in Eq. (27) as

$$\tilde{m} \sim O(\sqrt[4]{N_c}). \quad (32)$$

By using Eqs. (29), (31) and (32) for the matrix elements in Eq. (28), we eventually get the Complex 2D Matrix Model for a_1 meson with N_c dependence factored out by λ as

$$H(\lambda) = \begin{pmatrix} \frac{1}{\lambda^2} \sqrt{s_p} & \frac{\lambda}{2\tilde{m}} \sqrt{Z} v_{a_1 \pi \rho} \\ \frac{\lambda}{2\tilde{m}} \sqrt{Z} v_{a_1 \pi \rho} & m_{a_1} \end{pmatrix}, \quad (33)$$

$$\lambda \equiv \sqrt[4]{3/N_c}, \quad (34)$$

where $\sqrt{s_p}$, \sqrt{Z} , $v_{a_1 \pi \rho}$ and \tilde{m} in (33) are the constants estimated at $N_c = 3$ as shown above Eq. (27). $\frac{1}{\lambda^2} \sqrt{s_p}$ and m_{a_1} in Eq. (33) are the energies of the $\pi\rho$ -molecule state and the $q\bar{q}$ state, and they form the appropriate basis. The (1,1) element with negative power of λ reflects that a resonance state appears due to highly nonperturbative hadron dynamics.

Then, by applying the conditions (9) and (11) to the Hamiltonian (33), we can get the geometrical map on the complex- N_c plane for the a_1 meson in Fig. 6. (A prescription of writing geometrical maps is shown in Appendix B.) Six exceptional points and four transition lines, two of which are half-lines, appear on this map. These numbers can be derived from the power counting about λ in Eq. (12). The transition line shown by the solid curve can cross the real λ axis between $\lambda = 0$ ($N_c = \infty$) and $\lambda = 1$ ($N_c = 3$). The crossing point shows a critical color number for transition as $\lambda_t = \sqrt[4]{3/N_c} \sim 0.93$, i.e., $N_c \sim 4.0$. This result indicates that, with continuous change of N_c from ∞ to 3, the internal structures of two hadronic states can be exchanged in terms of appropriate basis $q\bar{q}$ and $\pi\rho$ -molecule at the critical color number $N_c \sim 4.0$. Such a critical color number with character exchange for the a_1 meson is also reported from the analysis of the pole residues in Ref. [26]. In this way, by looking into the existence of nature transition from the geometry on the complex- N_c plane, we can discuss the typical N_c -dependence of the internal structure of hadrons from $N_c = \infty$ to 3.

Finally, we check the stability of the present results, especially that of the appearance of the critical color number near $N_c = 3$, when corrections are made in the N_c -counting of Eq. (33). Below Eq. (28), we have adopted two approximations: i) $v_{\text{WT}} \sim s \times O(N_c^{-1})$ for $s \gg (m_\rho + m_\pi)^2$, and ii) neglecting the energy dependence of $G_{\pi\rho}$. These two are introduced to perform a simple N_c -counting of the matrix elements in Eq. (33) as a first study. By including effects of their energy dependence, the counting in Eq. (33) can be moderately

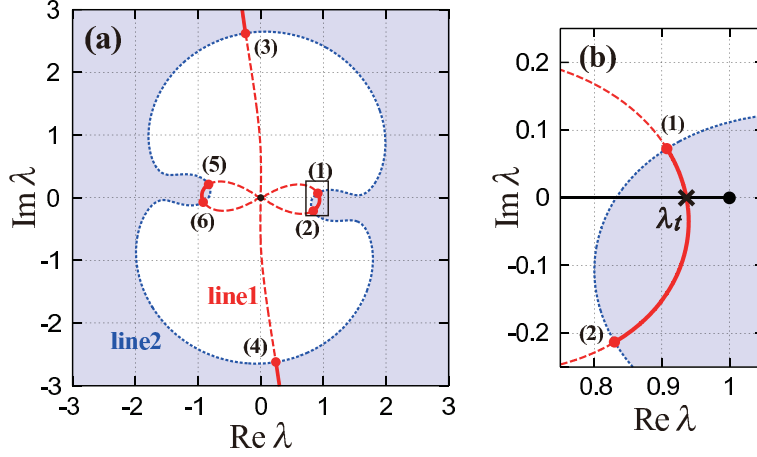


Fig. 6 (Color) (a) Geometrical map on the complex- N_c plane with $\lambda = \sqrt[4]{3/N_c}$. Constants in Eq. (33) are $\sqrt{s_p} = 1012 - 221i$, $m_{a_1} = 1189$, $\sqrt{Z} = 84 - 21i$ and $v_{a_1\pi\rho} = -6493$ in MeV unit. Line 1 and shaded area with the boundary of line 2 correspond to the conditions (9) and (11), respectively. Six exceptional points (n) ($n = 1 \sim 6$) as the crossing points between line 1 and line 2, and four transition lines as solid curves appear. (b) Close-up figure around a blank square in (a). Transition line as a solid curve crosses the real axis at $\lambda_t \sim 0.93$, i.e., $N_c \sim 4.0$, which locates between $\lambda = 0$ ($N_c = \infty$) and $\lambda = 1$ ($N_c = 3$).

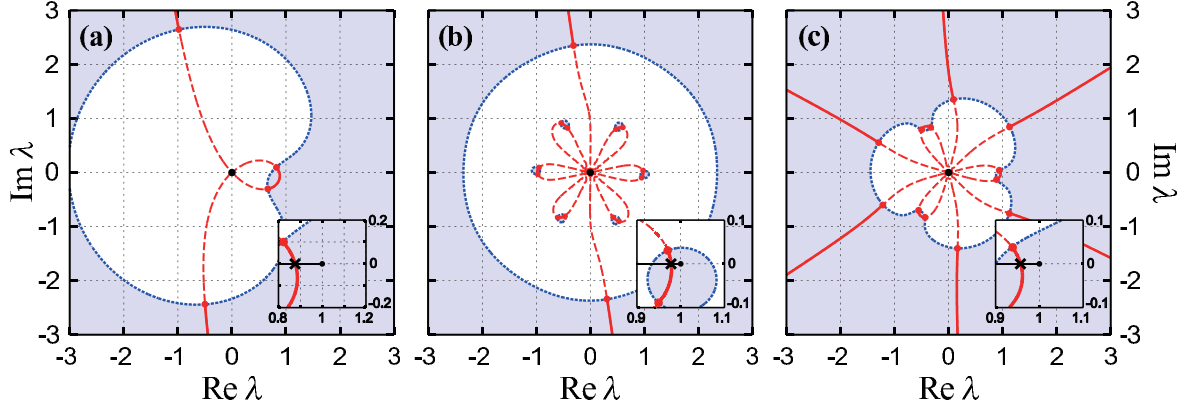


Fig. 7 (Color) Geometrical maps on the complex- N_c plane for (a) H_{-101} , (b) H_{-601} and (c) H_{-303} with same constants of Fig. 6. Notations for line 1, line 2, exceptional points and transition lines are also same as those in Fig. 6.

changed. First, Eq. (33) can be classified as H_{-201} of the PQR model (15). Now, there are three physical constraints; I) $P < 0$: mass and decay width of molecule resonance should increase at large- N_c , II) $Q = 0$: mass of $q\bar{q}$ is independent of N_c , and III) $R > 0$: QCD should become a free meson theory at large- N_c [11, 12]. With these constraints, we have checked various types of geometrical maps on the complex- N_c plane for physical sets of P , Q and R (For example, see Fig. 7 for H_{-101} , H_{-601} and H_{-303} as test cases). We find that the appearance of the critical color number near $N_c = 3$ in this paper is not so much affected by the corrections of the N_c -counting in Eq. (33). This is reasonably expected because $N_c = 3$ corresponds to the fixed point on the complex- N_c plane as discussed in the PQR model (15).

4. Summary and outlook

We have formulated the Complex 2D Matrix Model to get typical features about the parameter dependence of the internal structure of resonances. We suggest that the geometry on the complex-parameter space will give a simple criterion for the nature transition between resonance states within the real-parameter subspace. By applying the model to hadron physics, we have discussed the N_c -dependence of the internal structure of hadrons from the geometry on the complex- N_c plane. We show that, with continuous change of N_c from ∞ to 3, the internal structures of hadrons can be exchanged in terms of appropriate basis at the critical color number. We hope that the new concept of geometry on the complex- N_c plane and its possible topological classification will shed light on the exotic physics in QCD for the future.

Our model can be employed to general multi-level problems of resonances to analyze their internal structures with variation of a parameter in each system. Wide applications of our model to resonance physics are expected as a future prospect.

Acknowledgment

The authors thank Hiroki Nakamura, Koichi Yazaki, and Tetsuo Hyodo for their fruitful communications. The authors also thank Masuo Suzuki for his valuable suggestions during the international workshop ‘‘Resonances and non-Hermitian systems in quantum mechanics (2012)’’ in the Yukawa Institute for Theoretical Physics at Kyoto University. K. N. thanks Naomichi Hatano for his meaningful discussions about probabilistic interpretation of resonances. This work is supported by Grant-in-Aid for Scientific Research on Innovative Areas ‘‘Elucidation of New Hadrons with a Variety of Flavors’’ (Nos. 22105509 (K. N.), 22105510 (H. N.), 24105706 (D. J.) and E01:21105006 (A. H.)) from the Ministry of Education, Culture, Sports, Science, and Technology(MEXT) of Japan. K. N. is supported by the Special Postdoctoral Research Program of RIKEN.

A. Attaching number N_{at}

In this Appendix, we show line 1 always crosses the point $\lambda = 0$ for $R > 0$ in the PQR model. First, we calculate N_{at} showing how many times line 1 attaches to $\lambda = 0$. Eq. (9) can be written in the PQR model (15) as

$$\text{Re}[A(\lambda)^* \bar{V}(\lambda)] = \frac{1}{2} \text{Re}[(\Delta\varepsilon + \lambda^P v_{11} - \lambda^Q v_{22})^* \lambda^R \bar{v}] = 0, \quad (\text{A1})$$

with $\Delta\varepsilon \equiv \varepsilon_1^{(0)} - \varepsilon_2^{(0)}$ and $\bar{v}^2 \equiv v_{12}v_{21}$. We define $N_A \equiv \min(0, P, Q)$ to find a largest contribution within $A(\lambda)^*$ at $\lambda \rightarrow 0$. Then, at $\lambda \rightarrow 0$, Eq. (A1) becomes

$$\text{Re}[C(\lambda^{N_A})^* \lambda^R] = ar^{R+N_A} \text{Re} \left[e^{i\{(R-N_A)\theta + \phi\}} \right] = 0, \quad (\text{A2})$$

with $C \equiv ae^{i\phi}$ and $\lambda \equiv re^{i\theta}$. Now there are two cases as follows.

1) $R - N_A = 0$: By definition, $N_A \leq 0$ so that $R \leq 0$ and r^{R+N_A} becomes unity or divergent at $\lambda \rightarrow 0$. Therefore, Eq. (A2) is not satisfied at $\lambda = 0$, i.e., $N_{\text{at}} = 0$. Here we implicitly exclude the accidental case $\phi = \frac{\pi}{2} + n\pi$ ($n \in \mathbf{Z}$) which makes the equation indefinite.

2) $R - N_A \neq 0$: If the argument *strongly* approaches to certain angles at $\lambda \rightarrow 0$ as

$$(R - N_A)\theta + \phi \rightarrow \frac{\pi}{2} + n\pi, \quad (n \in \mathbf{Z}) \quad (\text{A3})$$

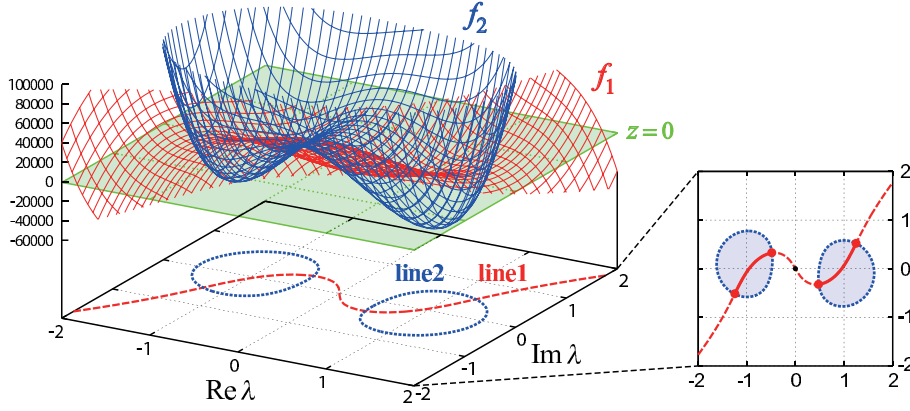


Fig. B1 (Color) Three dimensional plot of $z = f_i(x, y)$ ($i = 1, 2$) with contours at $z = 0$ (Left) and corresponding geometrical map (Right). Constants and powers of the matrix elements are same as those of Fig. 4(a).

Eq. (A2) is satisfied instead of possible divergence of r^{R+N_A} for $R + N_A < 0$. (A3) is equal to

$$\theta \rightarrow \frac{\frac{\pi}{2} - \phi}{R - N_A} + n \frac{\pi}{R - N_A}, \quad (n \in \mathbf{Z}) \quad (\text{A4})$$

Therefore $\Delta\theta \equiv \frac{\pi}{|R - N_A|}$ is an angle between nearest-neighboring two segments of line 1 near $\lambda = 0$. N_{at} is given by

$$N_{\text{at}} = \frac{2\pi}{\Delta\theta} = 2|R - N_A| = 2|R - \min(0, P, Q)|. \quad (\text{A5})$$

In table I, we summarize N_{at} for various sets of (P, Q, R) discussed in Figs. 2, 4, 6 and 7.

TABLE I: N_{at} for various sets of (P, Q, R)

	H_{111}	H_{221}	H_{233}	H_{151}	H_{-201}	H_{-101}	H_{-601}	H_{-303}
N_{at}	2	2	6	2	6	4	14	12

N_{at} in table I is consistent with the resultant geometry of line 1 around $\lambda = 0$ in Figs. 2, 4, 6 and 7.

Now, if $R > 0$ consistently with $V_{ij}(0) = 0$ in Eq. (1), $R - N_A \neq 0$ because $N_A \leq 0$. Therefore $N_{\text{at}} > 0$ and line 1 always crosses $\lambda = 0$.

B. Prescription of geometrical maps

In this Appendix, we show a prescription of writing geometrical maps. Eq. (9) and a boundary of Eq. (11) can be rewritten as algebraic equations:

$$f_i(\text{Re}\lambda, \text{Im}\lambda) = 0, \quad (\text{B1})$$

where f_i is a real function of $\lambda \in \mathbf{C}$ and $i = 1$ ($i = 2$) corresponds to Eq. (9) (boundary of Eq. (11)). By drawing a three-dimensional plot of $z = f_i(x, y)$, contours at $z = 0$ correspond to line 1 (for $i = 1$) and line 2 (for $i = 2$) (See, e.g., Fig. B1). In this way, by using a contour method, one can get geometrical maps without numerically solving the high-powered algebraic equations (9) and (11).

References

- [1] P. Ring and P. Schuck, *The Nuclear Many-Body Problem* (Springer, Berlin, 1980).
- [2] M. Born and J. R. Oppenheimer, *Ann. Phys.* **84**, 457 (1927).
- [3] H. A. Bethe, *Phys. Rev. Lett.* **56**, 1305 (1986).
- [4] J. V. Neumann and E. Wigner, *Phys. Z.* **30**, 467 (1929).
- [5] N. Moiseyev, *Non-Hermitian Quantum Mechanics* (Cambridge University Press, New York, 2011).
- [6] H. Feshbach, *Ann. Phys. (N.Y.)* **5**, 357 (1958); *Ann. Phys. (N.Y.)* **19**, 287 (1962).
- [7] I. Rotter, *J. Phys. A* **42**, 153001 (2009).
- [8] K. Sasada, N. Hatano and G. Ordóñez, *J. Phys. Soc. Jpn.* **80**, 104707 (2011).
- [9] E. Hernández and A. Mondragón, *Phys. Lett. B* **326**, 1 (1994).
- [10] Y. Nambu, in *Preludes in Theoretical Physics*, in honor of V. F. Weisskopf (North-Holland, Amsterdam, 1966).
- [11] G. 'tHooft, *Nucl. Phys. B* **72**, 461 (1974); *B* **75**, 461 (1974).
- [12] E. Witten, *Nucl. Phys. B* **160**, 57 (1979).
- [13] J. R. Peláez and G. Ríos, *Acta Phys. Pol. B* **2**, 215 (2009); L. S. Geng, E. Oset, J. R. Peláez and L. Roca, *Eur. Phys. J. A* **39**, 81 (2009).
- [14] T. Sakai and S. Sugimoto, *Prog. Theor. Phys.* **113**, 843 (2005); **114**, 1083 (2006).
- [15] For a phenomenological review: K. Nawa, H. Suganuma and T. Kojo, *Phys. Rev. D* **75**, 086003 (2007).
- [16] N. Hokkyo, *Prog. Theor. Phys.* **33**, 1116 (1965).
- [17] T. Berggren, *Nucl. Phys. A* **109**, 265 (1968).
- [18] W. Romo, *Nucl. Phys. A* **116**, 618 (1968).
- [19] T. Berggren, *Phys. Lett. B* **33**, 547 (1970).
- [20] N. Hatano, K. Sasada, H. Nakamura and T. Petrosky, *Prog. Theor. Phys.* **119**, 187 (2008); N. Hatano, T. Kawamoto and J. Feinberg, *Pramana* **73**, 553 (2009) (arXiv:0904.1044[quant-ph]).
- [21] T. Kato, *Perturbation Theory of Linear Operators* (Springer, Berlin, 1966).
- [22] W. D. Heiss and A. L. Sannino, *Phys. Rev. A* **43**, 4159 (1991); W. D. Heiss, *Phys. Rev. E* **61**, 929 (2000).
- [23] C. Dembowski, H. -D. Gräf, H. L. Harney, A. Heine, W. D. Heiss, H. Rehfeld and A. Richter, *Phys. Rev. Lett.* **86**, 787 (2001).
- [24] L. Roca, E. Oset and J. Singh, *Phys. Rev. D* **72**, 014002 (2005).
- [25] M. F. M. Lutz and E. E. Kolomeitsev, *Nucl. Phys. A* **730**, 392 (2004).
- [26] H. Nagahiro, K. Nawa, S. Ozaki, D. Jido and A. Hosaka, *Phys. Rev. D* **83**, 111504(R) (2011).
- [27] T. Hyodo, D. Jido and A. Hosaka, *Phys. Rev. C* **78**, 025203 (2008).
- [28] If N_c -dependent cut-off [13] is considered, $G_{\pi\rho}$ would have complicated N_c -dependence (even in a non-analytic way). In our present study, to simply perform the analytic continuation into the complex- N_c plane, we alternatively use N_c -independent cut-off corresponding to the mass scale of $q\bar{q}$ meson, which is also suggested as another candidate in Ref. [13].